
Agenda item:	7.3.1 High Speed Downlink Packet Data Access
Source:	Lucent Technologies
Title:	Overview of Multiple-Input Multiple-Output Techniques for HSDPA
Document for:	Discussion

1. INTRODUCTION

Recent information theoretic results show that by using multiple antennas at the transmitter and receiver, the capacity of a wireless channel can far exceed that of both a conventional system with single antennas at the transmitter and receiver and a diversity system which employs multiple antennas for diversity transmission and/or diversity reception [1]. Motivated by these results, a contribution [2] in the RAN1 working group introduced the use of multiple antennas at both the node B and at the terminal for efficiently providing high speed data packet access (HSDPA) on the downlink shared channel (DSCH). Additional contributions addressed the link performance [3,4,5], system performance [6] and complexity [7,8] of these multiple-input multiple-output (MIMO) systems. In this document, we give an overview and summary of these contributions, with an emphasis on the concepts that have been included in the HSDPA Technical Report [9].

2. TRANSMISSION TECHNIQUE

High data rates are achieved in the DSCH using the principle of multicode transmission where a single high speed data stream is demultiplexed into several lower rate substreams, and each of these lower rate substreams is modulated by a distinct spreading code. The high speed data stream has been channel coded, interleaved, and symbol mapped prior to demultiplexing. In a conventional single antenna system, this data stream is demultiplexed into N lower rate substreams, and the n th substream ($n = 1 \dots N$) is spread with spreading code n (where the spreading codes indexed by $n = 1 \dots N$ are mutually orthogonal). These substreams are summed together, scrambled and transmitted. A MIMO system transmitter with M antennas is shown in Figure 1. The high data rate source is demultiplexed into MN substreams, and the n th group ($n = 1 \dots N$) of M substreams is spread by the n th spreading code. The m th substream ($m = 1 \dots M$) of this group is transmitted over the m th antenna so that the substreams sharing the same code are transmitted over different antennas. These M substreams sharing the same code can be distinguished based on their spatial characteristics at the receiver using multiple antennas and spatial signal processing. Typically, the receiver must have at least M antennas to detect the signals sufficiently well; however, it is possible to perform detection using fewer than M antennas if more sophisticated detection algorithms are used.

Table 1 below lists the architectures for achieving a representative sample of data rates. By re-using the same spreading code over the transmit antennas, a MIMO system can achieve high data rates using smaller constellations compared to single antenna transmitters. For example, to achieve 10.8 Mbps, a single antenna transmitter requires 64QAM modulation whereas a MIMO transmitter with 4 antennas requires QPSK modulation. Because of the substream interference caused by code re-use, the MIMO techniques are used only when the code space is fully loaded. Otherwise, for a given spreading factor, a higher data rate can be achieved simply by using additional spreading codes.

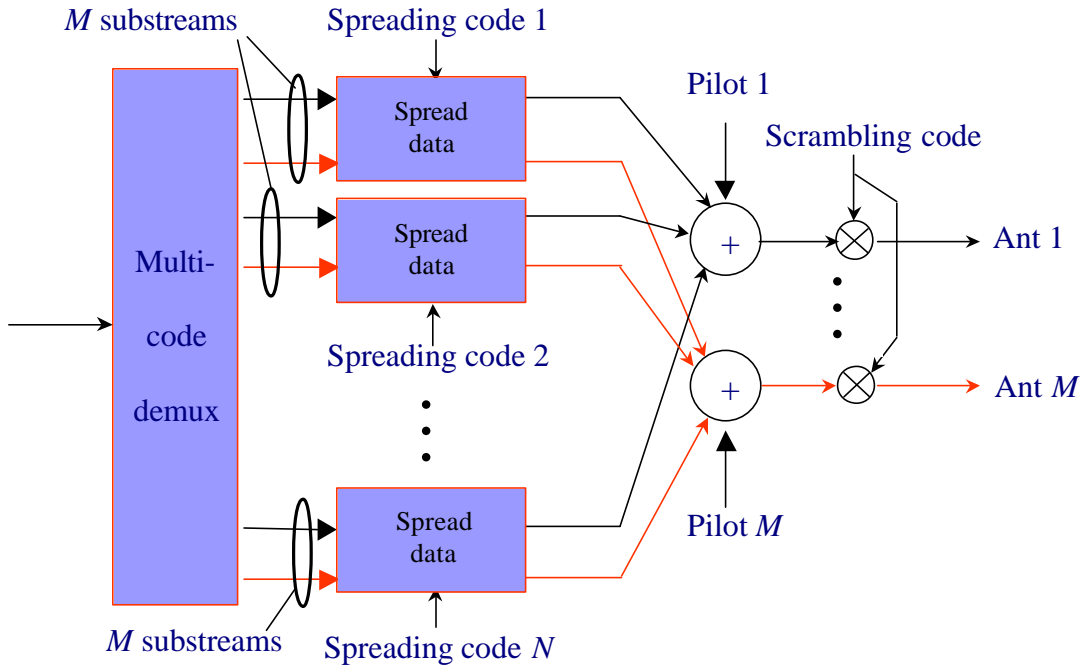


Figure 1.

# transmitters	Tx technique	Code rate	Modulation	Data rate per substream	# sub-streams	Total data rate
1	Conventional	$\frac{3}{4}$	64QAM	540Kbps	20	10.8Mbps
2	MIMO	$\frac{3}{4}$	8PSK	270Kbps	40	10.8Mbps
2	MIMO	$\frac{3}{4}$	16QAM	360Kbps	40	14.4Mbps
4	MIMO	$\sim\frac{1}{2}$	QPSK	135Kbps	80	10.8Mbps
4	MIMO	$\frac{3}{4}$	QPSK	180Kbps	80	14.4Mbps
4	MIMO	$\frac{3}{4}$	8PSK	270Kbps	80	21.6Mbps

Table 1. Antenna architectures

3. RECEIVER ARCHITECTURE

The MIMO architecture relies on multiple antennas at the terminal to distinguish the substreams sharing the same codes based on their spatial characteristics. The multiple antennas also provide diversity and combining gains which are beneficial for non-MIMO transmission. Following demodulation of the received RF signals to baseband, each antenna is followed a bank of filters matched to the N spreading codes. Assuming that the channel is flat fading, each group of M substreams sharing a given spreading code is orthogonal to the other substreams modulated with the other spreading codes. Following despreading, N parallel

space-time processors are used, each for demodulating M substreams sharing the same code. Examples of the space-time processor are a maximum likelihood detector and a V-BLAST detector [10] which employs a front-end linear transformation followed by ordered successive interference cancellation. At the output of the space-time processors, the signals are multiplexed, demapped, deinterleaved, and decoded. In frequency selective fading channels, the groups of substreams sharing different codes are no longer orthogonal. More sophisticated detectors which account for this multipath interference are under investigation.

4. PERFORMANCE RESULTS FOR IDEAL CHANNEL CONDITIONS

Link level simulations were performed and the frame error rate (FER) versus I_{or}/I_{oc} were measured for a variety of system architectures. In this section, we study the performance under ideal channel conditions: slow doppler fading corresponding to 3km/hr, flat fading channels, uncorrelated spatial channels, and perfect channel knowledge at the receiver. We first compare the systems for a fixed data rate of 10.8 Mbps, the highest achievable proposed for the conventional single antenna transmitter. Let the notation (M,P) denote a system with M transmit antennas and P receive antennas. We compare three systems: a conventional (1,1) system, a (2,2) MIMO system, and a (4,4) MIMO system. We assume a chipping rate of 3.84 Mcips/sec, a spreading factor of 32 chips per coded symbol, $N = 20$ spreading codes. The coding and data constellations for each system are given by the appropriate rows of Table 1. A parallel concatenated turbo decoding with 8 decoding iterations was used. Puncturing for the (4,4) system is used to achieve 10.8 Mbps. Figure 2 below shows the FER versus I_{or}/I_{oc} . Compared to the conventional transmitter, there are gains of about 9dB and 16dB for the (2,2) and (4,4) systems, respectively, at 10% FER. The enormous performance gains are due to a combination of diversity, receiver combining gain, and increased spectral efficiency due to MIMO processing. We emphasize that these gains are achieved using the same code resources (20 codes) as the conventional transmitter.

Using MIMO techniques, the maximum data rate can increase to 14.4 for the (2,2) system and up to 21.6 Mbps for the (4,4) system. As seen in the Table 1, the constellation sizes are still smaller than those of the single antenna transmitter. From Figure 3, we observe that the required I_{or}/I_{oc} 's for these rates are less than that of the conventional system operating at 10.8Mbps.

One way to interpret the I_{or}/I_{oc} gains for MIMO is that the high data rates can be achieved with less transmit power. Alternatively, if the DSCH is transmitted at a fixed power, then the MIMO gains translate into the higher data rates being used over a larger fraction of the cell area. Under this assumption of a rate-controlled DSCH, a system level study employing a base station scheduler showed that the average sector throughput using a (4,4) MIMO system increases by a factor of 1.8 and 2.8 for proportional fair and maximum C/I scheduling, respectively, compared to a conventional (1,1) system [6]. We note that some of the assumptions used in the system simulations are not consistent with those in Annex B of the Technical Report.

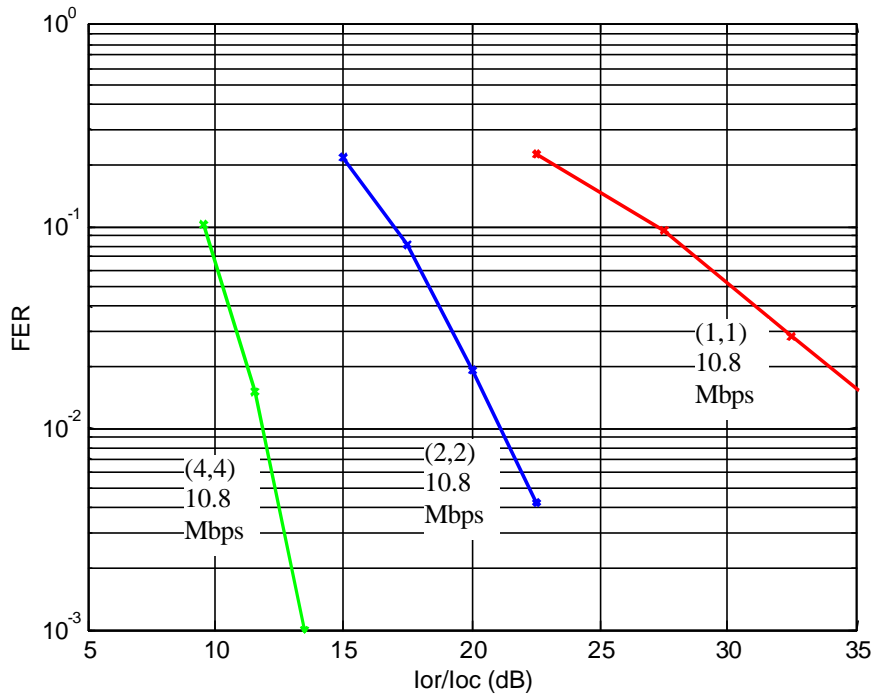


Figure 2. Frame error rates for 10.8 Mbps

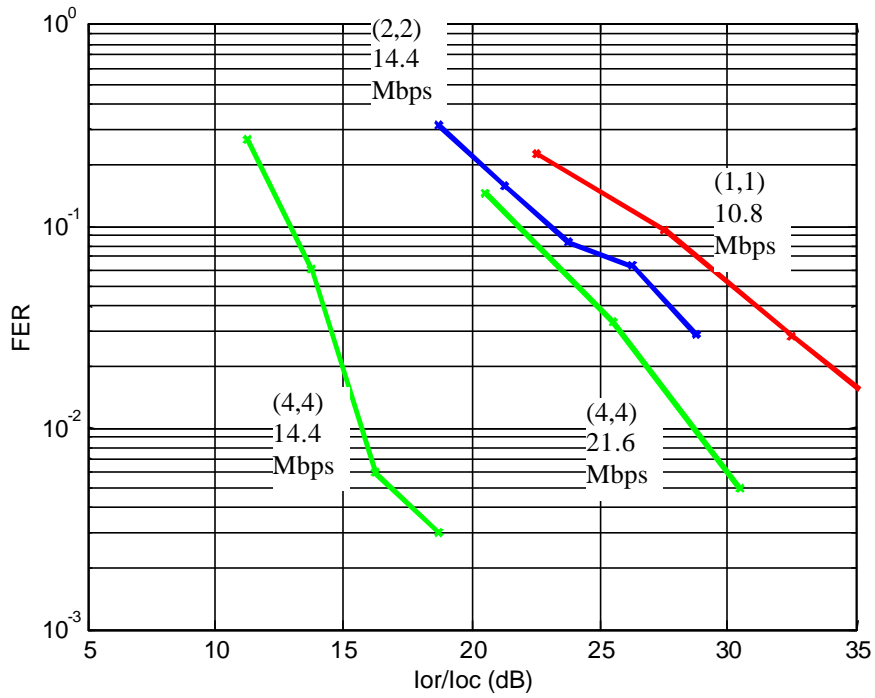


Figure 3. Frame error rates for data rates above 10.8Mbps

5. PERFORMANCE RESULTS FOR PRACTICAL CHANNELS CONDITIONS

In this section, we study the MIMO link level performance after removing the ideal assumptions from the previous section. Specifically, we study the effects of channel estimation, faster doppler fading, and correlated channels.

5.1 Channel Estimation

Each antenna transmits a code-multiplexed pilot channel with its N data channels, as shown in Figure 1. The data Walsh codes $W_1 \dots W_N$ are mutually orthogonal sequences of length 32, and the pilot Walsh codes $W_{p(1)} \dots W_{p(M)}$ are mutually orthogonal sequences of length 256 derived from a Walsh code of length 32 which is orthogonal to the data Walsh codes. (Recall that $N = 20$ so there are 12 remaining codes to choose from.) It follows that the data Walsh codes are orthogonal to each quarter of the pilot Walsh codes so that overall code orthogonality is maintained among pilot and data codes. The total pilot power is 10% of the total transmit power, and the pilots are equal power; hence for 2 and 4 antennas, each pilot is respectively 5% and 2.5% of the total transmit power. Additional overhead channels account for 10% of the total power, and the data traffic on the downlink shared channel accounts for the remaining 80%. Estimates of the channel coefficients $h_{m,p}$ are based on correlating the received signal with the pilot sequence. Each sequence is length 256 chips. Therefore in a 3.33ms frame at 3.84 Mcps, there are a total of 12800 chips per frame and 50 channel estimates per frame for each pair of transmit/receive antennas

Figure 4 shows the results for an uncorrelated channel at 3km/hr. The results for perfect channel knowledge were shown in [1] (except for the (2,2), 14.4Mbps case). With channel estimation, there is a slight degradation in performance for low E_b/N_0 , but at higher E_b/N_0 , the SNR of the pilot signals is also higher, resulting in less degradation. Figure 5 shows the results for faster doppler frequencies corresponding to a 30km/hr terminal. Increased time diversity acutally improves the performance of some system with respect to 3km/hr.

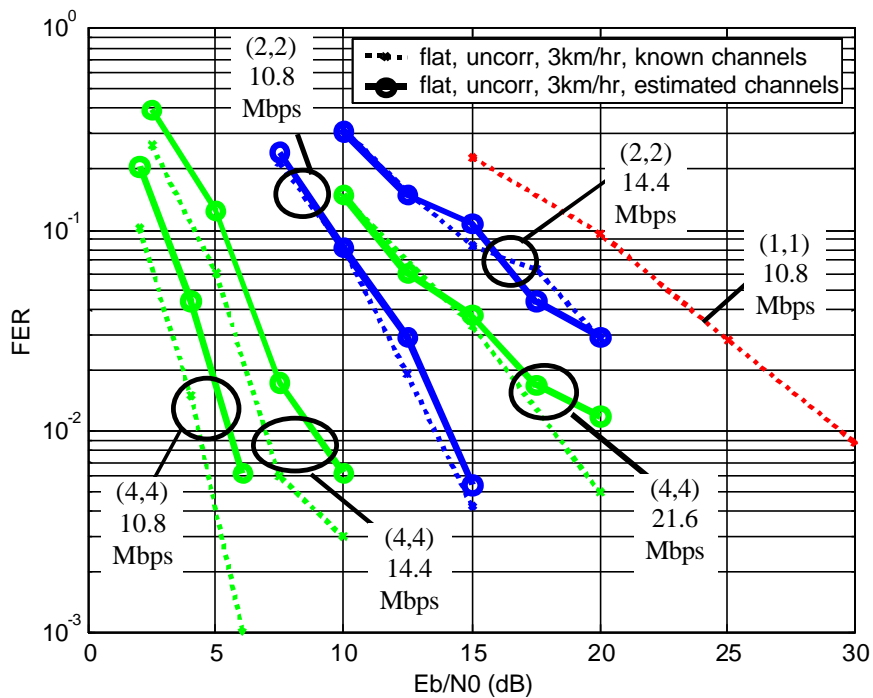


Figure 4. FER for flat fading, uncorrelated channels, 3km/hr

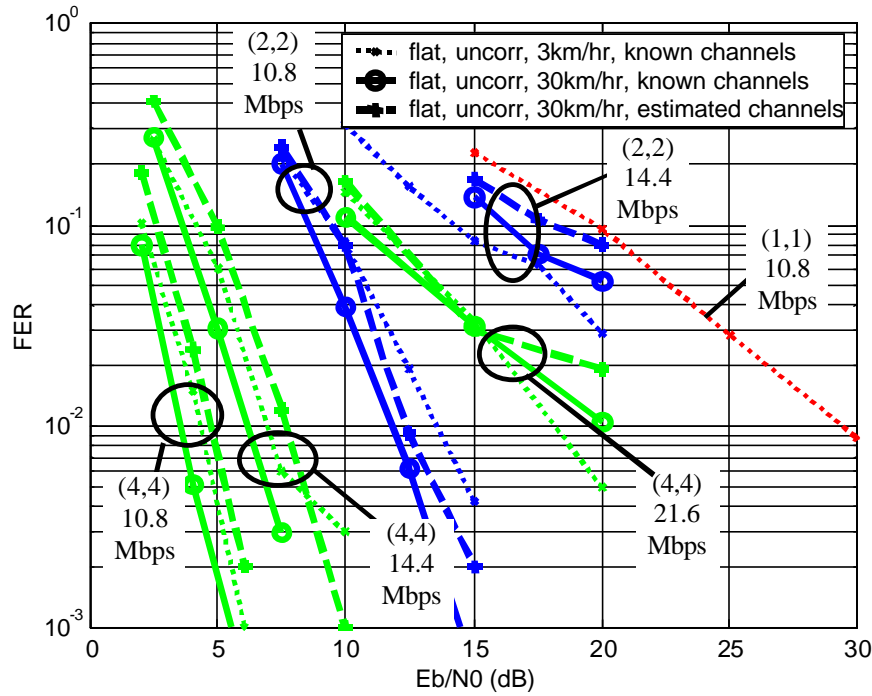


Figure 5. FER for flat fading, uncorrelated channels, 30km/hr

5.2 Channel Correlation

We now consider the effects of correlation between the antenna array elements at both the base station and terminal. In practical channels, correlation would occur if the scatterers surrounding the transmit and receive arrays do not provide sufficient richness. At the extreme when there is line of sight transmission between the arrays and there are no scatterers, then the signals are totally correlated. The correlation model is derived from [11] and is based on the illumination of elements from a ring of scatterers surrounding the receive array as shown in Figure 6. Let d_{BTS} and d_{UE} be the distance between antenna elements at the base station and terminal, respectively. The model assumes a uniform distribution of scatterers with angle $\mathbf{j} \in \{\mathbf{j}_{\min}, \mathbf{j}_{\max}\}$ around the base and $\mathbf{a} \in \{\mathbf{a}_{\min}, \mathbf{a}_{\max}\}$ around the terminal. The distances d_{BTS} and d_{UE} are small compared to the distance between the arrays and the distance between the scatterers and the arrays. Hence, each transmitter illuminates the same set of scatterers, and it follows that the correlation among the receive antennas is independent of the transmit antennas. Conversely, the correlation among the transmit antennas is independent of the receive antennas. Letting h_{mp} be the complex channel coefficient between transmitter m ($m = 1 \dots M$) and receiver p ($p = 1 \dots P$), the correlation between two coefficients is given by

$$E[h_{m_1 p_1} h_{m_2 p_2}^*] = E \left\{ \exp \left(j 2 \pi \frac{d(m_1, m_2) \sin \mathbf{j}}{\lambda} \right) \right\} E \left\{ \exp \left(j 2 \pi \frac{d(p_1, p_2) \sin \mathbf{a}}{\lambda} \right) \right\}$$

where $d(m_1, m_2)$ is the distance between transmit antennas m_1 and m_2 , $d(p_1, p_2)$ is the distance between receive antennas p_1 and p_2 , λ is the carrier wavelength, and the

expectations are taken with respect to the uniformly distributed angles $\mathbf{j} \in \{\mathbf{j}_{\min}, \mathbf{j}_{\max}\}$ and $\mathbf{a} \in \{\mathbf{a}_{\min}, \mathbf{a}_{\max}\}$. We consider urban and indoor channel models whose parameters are given in the table below.

	Urban	Indoor
d_{BTS}	10l	2l
d_{UE}	0.5l	0.5l
\mathbf{j}_{\min}	7.5°	-70°
\mathbf{j}_{\max}	52.5°	70°
\mathbf{a}_{\min}	0°	0°
\mathbf{a}_{\max}	360°	360°

Table 2. Parameters for correlated channels

For a (2,2) system, we define the channel vector $\mathbf{h} \triangleq [h_{11} \ h_{21} \ h_{12} \ h_{22}]^T$ (T denotes the matrix transpose) and the correlation matrix $\mathbf{R} \triangleq E[\mathbf{h}\mathbf{h}^H]$ (H denotes the Hermitian transpose). Then for the urban channel

$$\mathbf{R} = \begin{bmatrix} 1 & 0.05e^{-j2.3} & 0.30e^{-j3.1} & 0.01e^{j0.9} \\ 0.05e^{j2.3} & 1 & 0.01e^{-j0.9} & 0.30e^{-j3.1} \\ 0.30e^{j3.1} & 0.01e^{j0.9} & 1 & 0.05e^{-j2.3} \\ 0.01e^{-j0.9} & 0.30e^{j3.1} & 0.05e^{j2.3} & 1 \end{bmatrix},$$

and for the indoor channel,

$$\mathbf{R} = \begin{bmatrix} 1 & -0.07 & -0.30 & 0.02 \\ -0.07 & 1 & 0.02 & -0.30 \\ -0.30 & 0.02 & 1 & -0.07 \\ 0.02 & -0.30 & -0.07 & 1 \end{bmatrix}.$$

For an uncorrelated channels, \mathbf{R} is given by the identity matrix. Given the correlation matrix \mathbf{R} , the correlated channel coefficients \mathbf{h}_{corr} is given by $\mathbf{h}_{corr} = \mathbf{R}^{1/2}\mathbf{h}_{uncorr}$ where $\mathbf{R}^{1/2}$ is the matrix square root of \mathbf{R} , and \mathbf{h}_{uncorr} is the vector of uncorrelated channel coefficients. In the simulations, the components of \mathbf{h}_{uncorr} are independent zero-mean, complex Gaussian random

variables with unit energy whose time variations are governed by a Jakes fading process. For systems with 4 antenna, we assume linear arrays in computing the correlations.

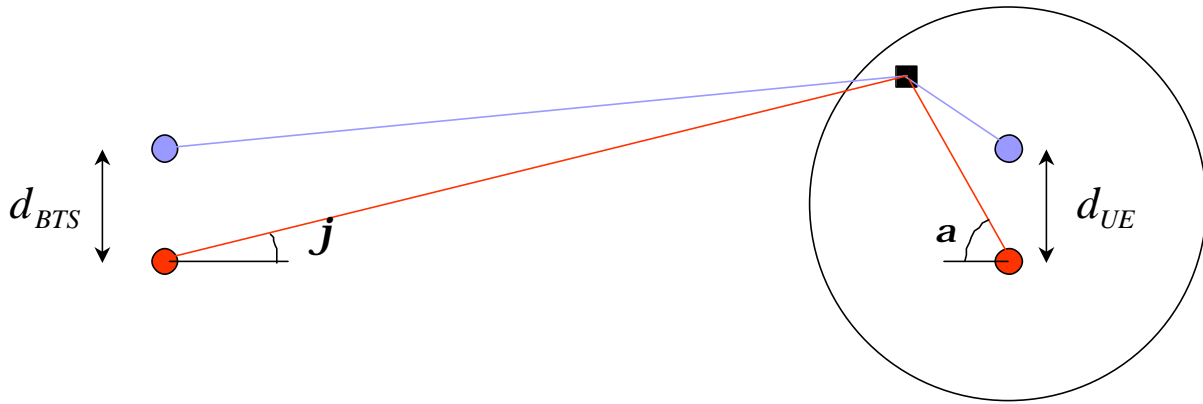


Figure 6. Model for deriving channel correlations

Figures 7 and 8 show the results for correlated channels. Under urban channel model, the degradation due to channel correlations is less than 1dB at 10% FER. For indoor channels, the loss is similar, indicating that base station antenna spacing of $2I$ does not degrade performance significantly as long as the angular spread around it is sufficient.

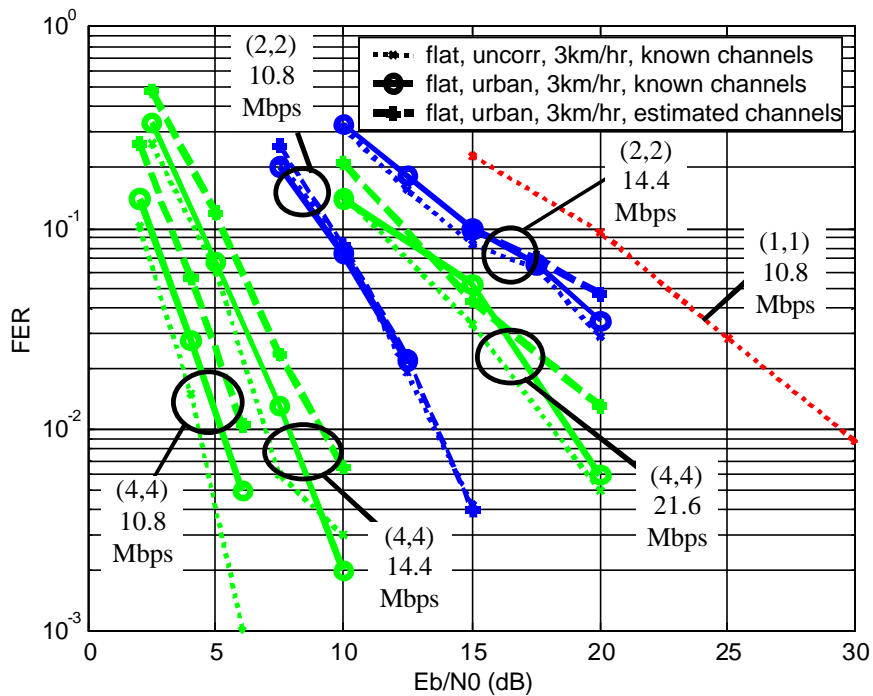


Figure 7. FER for flat fading, urban channels, 3km/hr

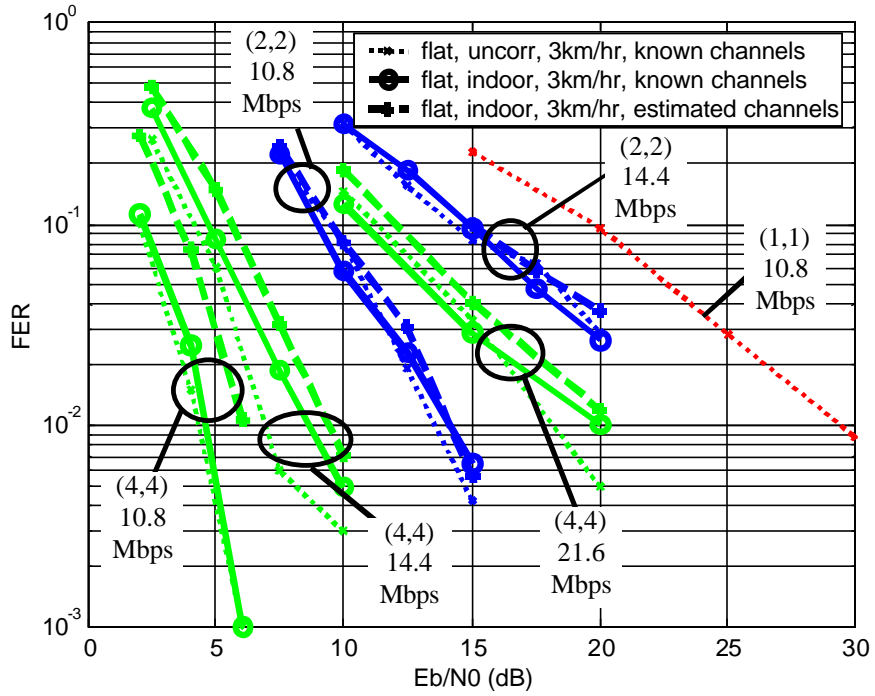


Figure 8. FER for flat fading, indoor channels, 3km/hr

We now consider the MIMO performance in even more highly correlated channels defined by Channels A and B below.

	Channel A	Channel B
d_{BTS}	0.3 <i>l</i>	0.2 <i>l</i>
d_{UE}	0.3 <i>l</i>	0.2 <i>l</i>
\mathbf{j}_{min}	0°	0°
\mathbf{j}_{max}	360°	360°
\mathbf{a}_{min}	0°	0°
\mathbf{a}_{max}	360°	360°
Avg. cross-corr (2,2)	0.22	0.57
Max. cross-corr (2,2)	0.29	0.64
Avg cross-corr. (4,4)	0.16	0.26
Max cross-corr. (4,4)	0.40	0.64

Table 3. Parameters for highly correlated channels

Figure 9 gives the performance for the (2,2) system at 10.8Mbps. As references, the red curve gives the performance of a conventional (1,1) system using 64QAM, and the green curve corresponds to a (2,2) system with uncorrelated channels. The performance in correlated channels is very robust. Under channel A, the performance degradation is negligible. With higher correlation in channel B, the performance loss is less than 2dB. Some of this performance loss is due to the loss in diversity which is inherent in any receiver with multiple antennas.

Figure 10 gives the performance of the (4,4) system at 10.8 Mbps. The red curve is the (1,1) reference, and the green curve is the performance of the (4,4) system in uncorrelated channels. The performance of the (4,4) system is not as robust to correlated channels due to unfavorable eigenvalue distribution of the correlation matrix \mathbf{R} . In other words, the low rank of the channel matrix results in poor performance of the detector. This problem can be solved by transmitting on fewer antennas to better match the rank of the channel. We choose to transmit with two antennas so that the rates and transmission techniques in Table 1 can be used. One would expect that transmitting on the two outer antennas would lead to the best performance. However, as shown by the dashed lines in Figure 3, the performance is satisfactory even if we transmit from the *worst* antenna pair (worst in the sense of highest average cross-correlation). Hence *any* antenna selection algorithm, even a random one, would result in better performance. Since a channel's angle spread is largely a function of the antenna heights and scatterer density, it will basically remain fixed for a given environment (e.g., urban or suburban). Therefore the channel correlations will also remain fixed. It follows that in situations with high channel correlation, the decision to operate in 'choose two of four antennas' mode could be done very infrequently, for example at call setup only, resulting in minimal control overhead.

Figure 11 gives the performance of the (4,4) system at 14.4 Mbps. As in the (4,4) 10.8Mbps case, the performance with four transmit antennas is sensitive to high channel correlations, but it can be significantly improved by transmitting with just two antennas.

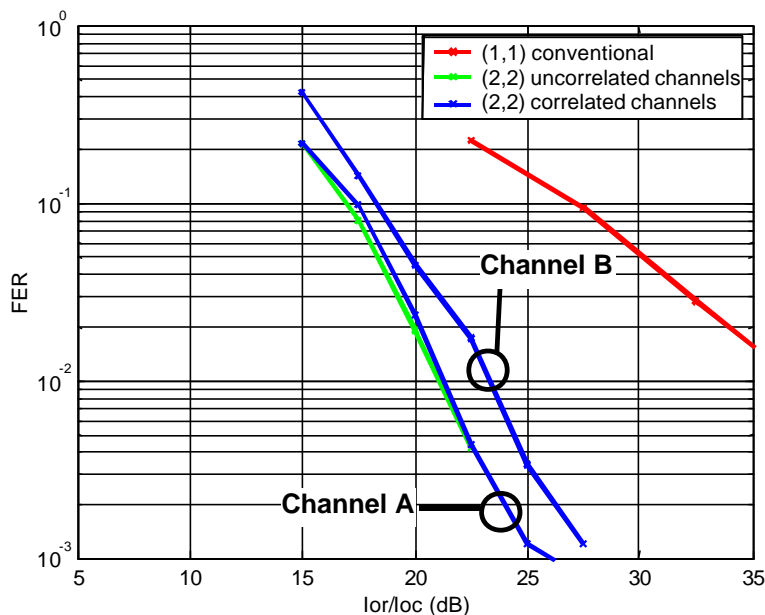


Figure 9. FER for (2,2) system, 10.8 Mbps

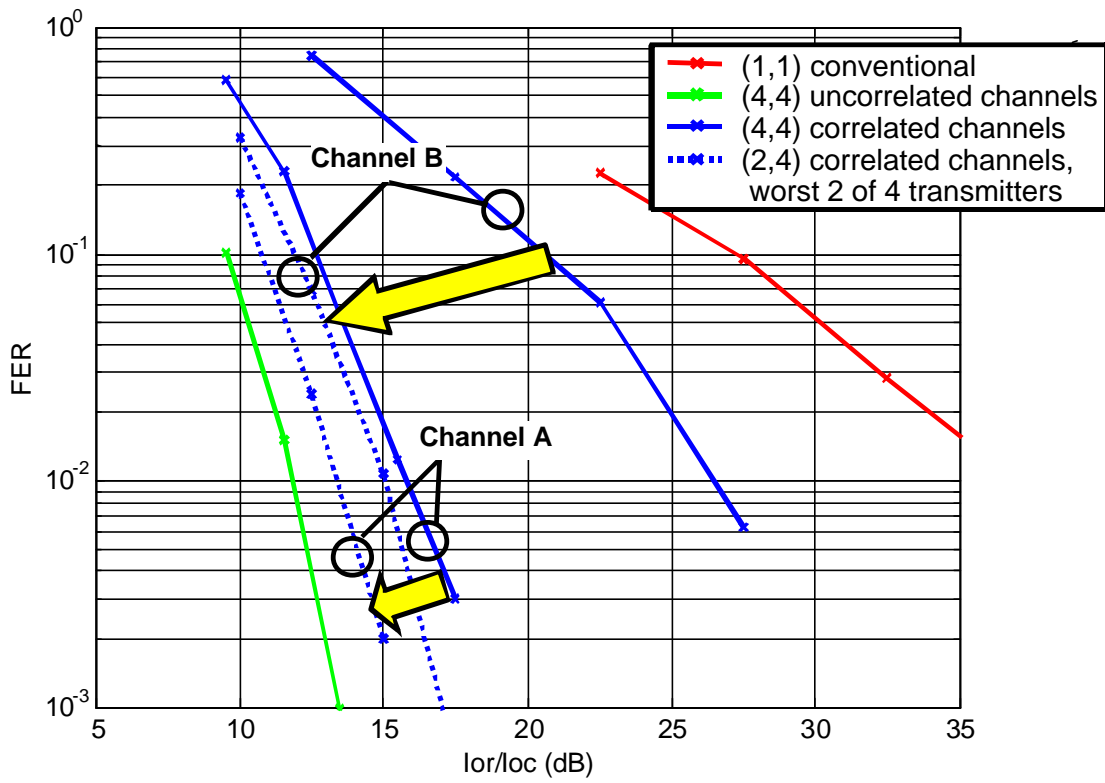


Figure 10. FER for (4,4) system, 10.8 Mbps

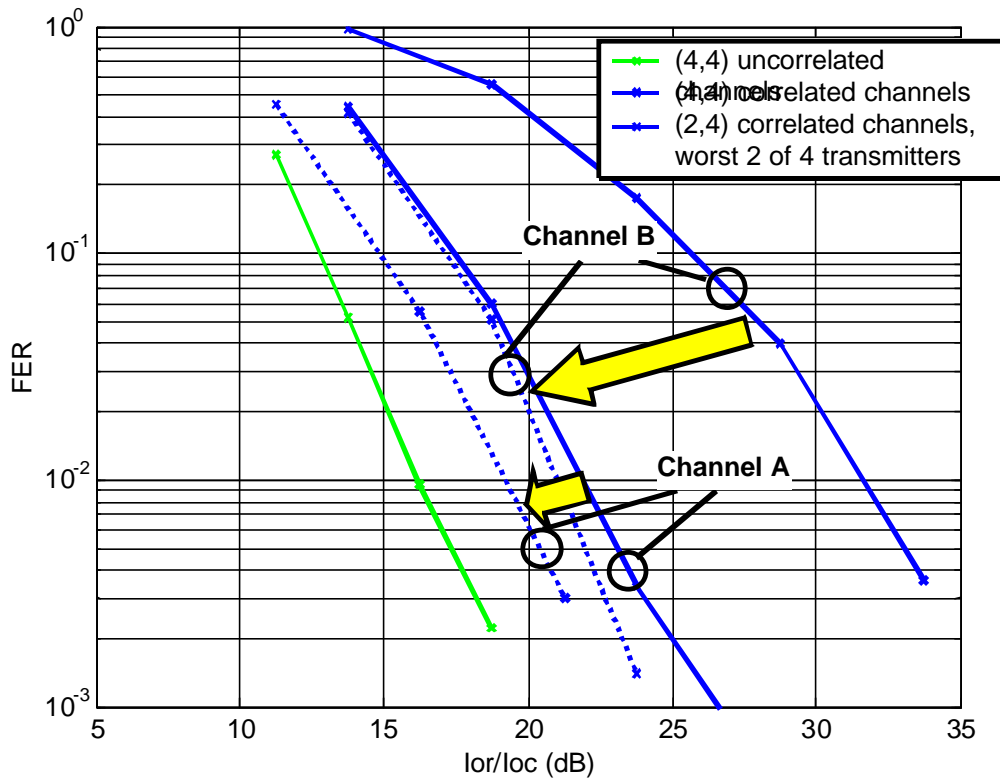


Figure 11. FER for (4,4) system, 14.4 Mbps

6. NODE B COMPLEXITY CONSIDERATIONS

The block diagram for M antenna MIMO HSDPA transmission is shown in Figure 1. A single antenna transmitter demultiplexes the high speed data stream into N lower rate substreams (N is the number of Walsh spreading codes) whereas the MIMO transmitter demultiplexes the stream into MN lower rate substreams. In terms of baseband processing, the MIMO demultiplexers require minimal additional complexity over the single antenna demultiplexers. For backwards compatibility, non-MIMO transmission on other dedicated channels are transmitted over antenna 1. The MIMO and non-MIMO signals will not interfere with each other since the Walsh codes used are mutually orthogonal. Similar to the case of transmit diversity with multiple antennas, orthogonal pilot sequences are transmitted from each antenna to allow for timing acquisition, synchronization, and/or channel estimation.

The power of the MIMO transmissions are normalized so that for the DSCH so the total transmit power summed across the M antennas is the same as for the single antenna transmission. Hence while multiple power amplifiers are required for MIMO transmission, (typically one per transmit antenna), the loading on any of these amplifiers will be reduced compared to the power amplifier in a single antenna system. Furthermore, because MIMO transmission uses smaller data constellations, the peak-to-average power ratio could also be reduced

In the same way that transmit diversity techniques rely on uncorrelated fading among pairs of transmitter and receiver antennas, high spectral efficiencies of the MIMO system also rely on uncorrelated fading. The correlation depends on the spacing between antennas and height of the antennas with respect to the local scatterers. For outdoor base stations where the antennas are significantly higher than the scatterers, totally uncorrelated fading is achieved using a separation of 10 wavelengths between nearest neighbors in a linear base array of dual-polarized antennas [12]. For indoor base stations, or in situations where the antennas are at the same height as the local scatterers, the scatterers will cause more decoupling of the signals at the antennas. Hence the required antenna separation for a given level of correlation will be even less.

7. UE COMPLEXITY CONSIDERATIONS

The MIMO UE will require multiple uncorrelated antennas and additional baseband processing to perform space-time combining and spatial processing on substreams which share the same code. In contrast to the Node B which is typically above the level of the local scatterers, the terminal receiver is usually at the same level as local scatterers. Because of these scatterers, a smaller antenna spacing of $\frac{1}{2}$ wavelength is sufficient to achieve decorrelation among the multipath signals, particularly in cases in which there is no direct path between receiver and transmitter (Rayleigh fading) [12]. However, the final correlation could be affected by factors such as proximity to the human body and other objects

With regard to RF complexity, for a terminal with M antennas, where M is assumed to be 2 or 4, one could simply replicate the conventional RF/IF chain M times and perform baseband combining. However, one may potentially lower the complexity by performing combining in RF or using a homodyne chip solution. In performing combining in RF, the UE cost can be reduced by using a single IF chain and by omitting baseband combiners. Using homodyne chip technology, the entire RF/IF chain is implemented in silicon, resulting in significantly

reduced cost. The practicality of these emerging technologies needs to be investigated with respect to cost and complexity.

As mentioned above in Section 3, additional baseband processing is required at the UE terminal for performing space-time processing. The main baseband components are a bank of despanders, a set of detectors for eliminating spatial interference, and a turbo decoder. It was shown that the turbo decoder requires the majority of the processing power. For a 2 transmit antenna, 2 receive antenna system, the detector portion accounts for about 5% of the total processing and the turbo decoder accounts for about 85% of the processing. For a 4 transmitter, 4 receiver system, the detector and turbo decoder account for about 20% and 70% respectively of the total processing. Compared to a conventional single antenna receiver for HSDPA which requires about 1.6×10^9 operations per second, the 2 antenna receiver requires 3.3×10^9 operations per second and the 4 antenna receiver requires 7.9×10^9 operations per second. These computational requirements were estimated assuming brute-force processing techniques but are already within the range of existing hardware technologies. More detailed studies will mostly likely reduce the processing requirements significantly.

8. REFERENCES

- [1] G. J. Foschini and M. J. Gans, On limits of wireless communication in a fading environment when using multiple antennas, *Wireless Personal Communications*, vol. 6, no. 3, pp 311-335, March 1998.
- [2] Lucent. Enhancements for HSDPA Using Multiple Antennas. TSG_R WG1 document TSGR1#15(00)1096, 22-26th, August 2000, Berlin, Germany.
- [3] Lucent. Preliminary link level results for HSDPA using multiple antennas. TSG_R WG1 document TSGR1#16(00)1218, 10-13th, October 2000, Pusan, Korea.
- [4] Lucent. Further link level results for HSDPA using multiple antennas. TSG_R WG1 document TSGR1#17(00)1386, 21-24th, November 2000, Stockholm, Sweden.
- [5] Lucent. Link level results for HSDPA using multiple antennas in correlated channels. TSG_R WG1 document TSGR1#18(01)0131, 15-19th, January 2001, Boston, USA.
- [6] Lucent. Throughput simulations for MIMO and transmit diversity enhancements to HSDPA. TSGR1#17(00)1388, 21-24th, November 2000, Stockholm, Sweden.
- [7] Lucent. Practical aspects of multiple antenna architectures for HSDPA. TSG_R WG1 document TSGR1#16(00)1219, 10-13th, October 2000, Pusan, Korea.
- [8] Lucent. Complexity of Node B for MIMO architectures. TSG_R WG1 document TSGR1#18(01)0134, 15-19th, January 2001, Boston, USA.
- [9] 3rd Generation Partnership Project; Technical Specification Group Radio Access Network; Physical Layer Aspects of UTRA High Speed Downlink Packet Access; (Release 2000), (3G Technical Report (TR) 25.848, version 0.2.1), Tdoc R1-01-0168, TSG-RAN WG1; January 15th-18th, 2001, Boston, USA.
- [10] G.J. Foschini, G.D. Golden, R.A. Valenzuela and P.W. Wolniansky, Simplified processing for high spectral efficiency wireless communication employing multi-element arrays. *IEEE Journal on Selected Areas in Communications*, vol. 17, no. 11, pp 1841-1852, November 1999.
- [11] Siemens. Channel model for TX diversity simulations using correlated antennas. TSG_R WG1 document TSG1#15(00)1067, 22-25th, August 2000, Berlin, Germany.
- [12] D. Chizhik, F. Rashid-Farrokhi, J. Ling, A. Lozano, "Effect of antenna separation on the capacity of BLAST in correlated channels," *IEEE Communications Letters*, vol. 4, no. 11, pp. 337-339, November 2000.